A New Bridging Ligand for the $[Mo_2]^{4+}$ Dimer: Syntheses and X-ray Crystal Structures of the Redox Pair $[Mo_2\{\mu\text{-}\eta^2\text{-}(NPh)_2CNHPh\}_4]^{0/+}$

Philip J. Bailey,* Simon F. Bone, Lindsey A. Mitchell, Simon Parsons, Kenneth J. Taylor, and Lesley J. Yellowlees

Department of Chemistry, The University of Edinburgh, The King's Buildings, West Mains Road, Edinburgh EH9 3JJ, U.K.

Received June 14, 1996[⊗]

The quadruply bonded molybdenum dimer $[Mo_2\{\mu\text{-}\eta^2\text{-}(NPh)_2CNHPh\}_4]$ (**1**), bridged by four triphenylguanidine anion (guanidino) ligands, has been synthesized and structurally characterized. The guanidino ligands greatly stabilize the oxidized forms of this complex, and it is reversibly oxidized to the red monocation and the blue dication at readily accessible potentials ($E_{1/2} = -0.05$ and $+0.85$ V *vs* Ag/AgCl, respectively). The $[Mo_2\{\mu\text{-}\eta^2\text{-}(NPh)_2CNHPh\}_4]^+$ cation (**2**) has also been structurally characterized as its $[BF_4]^-$ salt showing that the Mo−Mo distance increases from 2.0839(9) to 2.2902(12) Å on oxidation, an unprecedented increase for such systems and almost 4 times that previously observed for a $[Mo_2]^{4+/5+}$ pair. The N−Mo−Mo−N torsion angle is also found to increase from 4.5 to 7.6° on oxidation. The crystallographic data are as follows. **1**·2.2Et_2O: $C_{84.8}H_{86}Mo_2N_{12}O_{2.2}$, monoclinic, *P*2/*n*, $a = 13.127(3)$ Å, $b = 14.335(3)$ Å, $c = 22.752(3)$ Å, $\beta = 90.434(13)°$, $Z = 2$. **2**$[BF_4]^-$·3CH_2Cl_2: $C_{79}H_{70}BCl_6F_4Mo_2N_{12}$, monoclinic, $P2_1/c$, $a = 13.426(3)$ Å, $b = 23.693(7)$ Å, $c = 23.573(7)$ Å, $\beta = 92.93(2)°$, $Z = 4$.

Introduction

The $[Mo_2]^{4+}$ unit has been structurally characterized with a wide range of anionic ligands bridging the metal centers.[1] Possibly the most common of these ligands are the carboxylate anions and their various nitrogen analogs. During the course of a study of the ligand properties of guanidine anions,[2] we have found that monodeprotonated guanidines can act as chelating guanidino ligands.[3] We surmised that, given their steric and electronic relationships to carboxylates, these anions might equally well bridge a molybdenum dimer and furthermore exhibit interesting electronic properties by virtue of the delocalization of their uncoordinated nitrogen lone pair into the ligand π-system. Such a delocalization leads to the possibility of a second resonance form for the ligand (Figure 1), which would result in an enhancement of the ligand basicity and hence its ability to stabilize higher oxidation states.

Experimental Section

All reactions and manipulations were carried out under an atmosphere of dry, oxygen-free nitrogen using standard Schlenk techniques and solvents which were distilled from appropriate drying agents under nitrogen immediately prior to use. Molybdenum hexacarbonyl and silver tetrafluoroborate were purchased from Aldrich and used without further purification. Triphenylguanidine was prepared by condensation of aniline with diphenylcarbodiimide in THF under reflux. NMR spectra were recorded on a Bruker AC 250 spectrometer, and EPR spectra, on a Bruker ER 200D-SRC spectrometer. Mass spectra were recorded on a Kratos MS50 TC instrument in the positive ion FAB mode using 3-nitrobenzyl alcohol as matrix and CsI as calibrant.

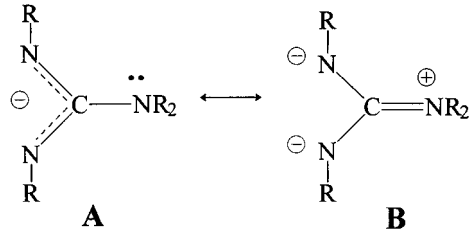

Figure 1. Resonance structures for a guanidino ligand.

Electrochemical measurements were performed using GPES version 4 software run on a personal computer connected to an Autolab system via a PSTAT 10 potentiostat. Cyclic voltammetry was performed using a standard three-electrode configuration with platinum working (0.5 mm diameter disk) and counter electrodes and a Ag/AgCl reference which gave the $CpFe/CpFe^+$ couple at 0.62 V. Bulk electrolyses were executed in an "H-type" cell with platinum basket and mesh as working and counter electrodes, respectively. All measurements were made in a nitrogen-purged solution of CH_2Cl_2/0.5M [*n*-Bu_4N][BF_4]. *In situ* UV/vis/near-IR spectroelectrochemistry was performed on solutions in CH_2Cl_2/0.5M [*n*-Bu_4N][BF_4] at 0 °C and at an optically transparent electrode (OTE) in a Perkin-Elmer Lambda 9 spectrometer.[4] After each redox step, the starting material was regenerated to confirm full chemical reversibility.

Preparation of $[Mo_2\{\mu\text{-}\eta^2\text{-}(NPh)_2CNHPh\}_4]$ (1). $Mo(CO)_6$ (1 g, 3.79 mmol) and 1,2,3-triphenylguanidine (2.055 g, 7.68 mmol) were heated to reflux in bis(2-methoxyethyl) ether (diglyme, 20 cm^3) under nitrogen for 6 h while sublimed $Mo(CO)_6$ was periodically returned to the solution by swirling of the flask. The resulting yellow/brown solution was allowed to cool slowly to ambient temperature and was then stored at −20 °C overnight. The resulting yellow crystalline material was collected by filtration under nitrogen, washed with ice-cold diethyl ether (3 × 5 cm^3), and dried under vacuum. Yield: 1.21 g, 48%. The yield of this reaction was found to depend critically upon the rigorous exclusion of oxygen from the system. ^1H NMR (250 MHz, $CDCl_3$, 20 °C, TMS): $\delta = 7.0$ (multiplet, 15H, Ph), 5.9 (s, br, 1H, NH). ^{13}C NMR (62.9 MHz, $CDCl_3$, 20 °C, TMS): $\delta = 149.7$ (CN_3), 141.7, 129.2, 128.5, 127.9, 124.6, 122.5, 120.3, 117.5. MS (+FAB),

[⊗] Abstract published in *Advance ACS Abstracts,* February 1, 1997.

(1) Cotton, F. A; Walton, R. A. *Multiple Bonds Between Metal Atoms,* 2nd ed.; Oxford University Press: New York, 1993; see also references therein.

(2) Bailey, P. J.; Blake, A. J.; Kryszczuk, M.; Parsons, S.; Reed, D. *J. Chem. Soc., Chem. Commun.* **1995**, 1647. Bailey, P. J.; Mitchell, L. A.; Raithby, P. R.; Rennie, M.-A.; Verhorevoort, K.; Wright, D. S. *Chem. Commun.* **1996**, 1351.

(3) Bailey, P. J.; Mitchell, L. A.; Parsons, S. *J. Chem. Soc., Dalton Trans.* **1996**, 2839.

(4) Heath, G. A.; Yellowlees, L. J.; Braterman, P. S. *J. Chem. Soc., Chem. Commun.* **1981**, 287.

S0020-1669(96)00712-4 CCC: $14.00

m/z (%): 1334 (100) [M^+], 1258 (6) [$M^+ - Ph$], 1245 (11) [$M^+ - NPh$], 1141 (13) [$M^+ - PhNCNPh$], 1052 (28) [$M^+ - (NPh)_2CNHPh$]. UV/vis (CH_2Cl_2 solution): $\nu = 24\,370$ cm^{-1} ($\epsilon = 9420$ mol^{-1} dm^3 cm^{-1}).

Preparation of [Mo$_2${μ-η^2-(NPh)$_2$CNHPh}$_4$][BF$_4$] (2). [Mo$_2${μ-η^2-(NPh)$_2$CNHPh}$_4$] (**1**) (0.25 g, 0.19 mmol) was dissolved in CH_2Cl_2 (10 cm^3), and solid $AgBF_4$ (0.041 g, 0.21 mmol) was added. The solution immediately changed color from yellow to deep red, was stirred for 1 h, and was then filtered through a short Celite column to remove precipitated silver. Layering of the resulting solution with hexane (10 cm^3) provided a crop of black, air-stable crystals after several days. The yield was 0.17 g (64%). EPR (CH_2Cl_2): $\nu = 9.79$ GHz, $T = 293$ K: $g_{iso} = 1.943$, $A_{iso} = 20.5 \times 10^{-4}$ cm^{-1}; $\nu = 9.46$ GHz, $T = 77$K: $g_{||} = 1.955$, $A_{||} = 31.0 \times 10^{-4}$ cm^{-1}, $g_\perp = 1.9385$, $A_\perp = 15.4 \times 10^{-4}$ cm^{-1}; $g_{av} = 1.944$, $A_{av} = 20.6 \times 10^{-4}$ cm^{-1}. UV/vis (CH_2Cl_2 solution): $\nu = 11\,900$ cm^{-1} ($\epsilon = 1330$ mol^{-1} dm^3 cm^{-1}), $\nu = 18\,900$ cm^{-1} ($\epsilon = 7120$ mol^{-1} dm^3 cm^{-1}), $\nu = 22\,710$ cm^{-1} ($\epsilon = 9430$ mol^{-1} dm^3 cm^{-1}), $\nu = 27\,320$ cm^{-1} ($\epsilon = 10\,500$ mol^{-1} dm^3 cm^{-1}).

Preparation of [Mo$_2${μ-η^2-(NPh)$_2$CNHPh}$_4$][BF$_4$]$_2$ (3). [Mo$_2${μ-η^2-(NPh)$_2$CNHPh}$_4$] (**1**) (0.25 g, 0.19 mmol) was dissolved in acetone (10 cm^3), and solid [NH$_4$]$_2$[Ce(NO$_3$)$_6$] (0.26 g, 0.47 mmol) was added. The solution immediately changed color from yellow to deep blue. Attempts at obtaining crystalline material from this solution have so far been hampered by the extreme sensitivity of **3** to reduction to **2**. UV/vis (CH_2Cl_2 solution): $\nu = 15\,010$ cm^{-1} ($\epsilon = 15\,910$ mol^{-1} dm^3 cm^{-1}), $\nu = 21\,400$ cm^{-1} ($\epsilon = 11\,590$ mol^{-1} dm^3 cm^{-1}).

X-ray Crystallography. Data for both crystals were collected on a Stoe Stadi-4 four-circle diffractometer equipped with an Oxford Cryosystems low-temperature device[5] operating at 150.0(2) K. Unit cell parameters for **1** were derived from 40 reflections ($30 < 2\theta < 32°$) and for **2** from 46 reflections ($26 < 2\theta < 28°$) measured at $\pm\omega$. Intensities were collected using $\omega-\theta$ scans in the ranges $5 < 2\theta < 50°$ for **1** and $5 < 2\theta < 45°$ for **2**. The data were corrected for absorption using ψ-scan data (transmission ranges 0.438−0.532 for **1** and 0.472−0.502 for **2**), and the structures were both solved by direct methods (SIR92).[6] Refinement was performed against F^2 using all data (SHELXTL)[7] with carbon-bound hydrogen atoms placed in calculated positions and treated according to a riding model. Hydrogen atoms bound to N in the guanidino ligands were located in difference maps and refined with similarity restraints on the N−H distances and U_{iso}(H) = 1.2U_{eq}(N) in the case of **1** but treated using a riding model in **2**. In **1**, the asymmetric unit contains one full-weight molecule of disordered diethyl ether. Difference maps implied that there were in addition several more molecules of this solvent, completely disordered about inversion centers with very low occupancy. Treatment of these regions in the manner described by van der Sluis and Spek[8] showed that these molecules contributed only 18.3 electrons per unit cell. For **1**, refinement converged with anisotropic displacement parameters on all non-hydrogen atoms to a conventional R1 of 6.12% [based on F and 4804 data with $F > 4\sigma(F)$] and wR2 = 16.16% (based on F^2 and all 7542 unique data) for 484 parameters. The corresponding parameters for **2** are R1 = 6.33% (5950 data) and wR2 = 14.12% (9855 data) for 937 parameters. The final difference synthesis maxima and minima were +0.80 and −0.65 e Å^{-3} for **1** and +0.61 and −0.48 e Å^{-3} for **2**. Structural data are available from the Cambridge Crystallographic Data Centre, 12 Union Road, Cambridge, CB2 1EZ, U.K. The results of crystallographic procedures are summarized in Table 1.

Table 1. Crystallographic Data for [Mo$_2${μ-η^2-(NPh)$_2$CNHPh}$_4$]·2.2Et$_2$O (**1**) and [Mo$_2${μ-η^2-(NPh)$_2$CNHPh}$_4$][BF$_4$]·3CH$_2$Cl$_2$ (**2**)

formula	$C_{84.8}H_{86}Mo_2N_{12}O_{2.2}$	$C_{79}H_{70}BCl_6F_4Mo_2N_{12}$
fw	1500.3	1678.86
space group	$P2/n$	$P2_1/c$
a, Å	13.177(3)	13.426(3)
b, Å	14.335(3)	23.693(7)
c, Å	22.752(3)	25.573(7)
α, deg	90	90
β, deg	90.434(13)	92.93(2)
γ, deg	90	90
V, Å^3	4281.2(14)	8124(4)
Z	2	4
T, K	152(2)	150(2)
λ, Å	0.710 73	0.710 73
ρ_{calc}, g cm^{-3}	1.152	1.373
μ(Mo Kα), cm^{-1}	3.42	5.65
R	0.0612	0.0633
R_w	0.1640[a,c]	0.1412[b,c]

[a] $w = 1/[\sigma^2(F_o^2) + (0.0867P)^2]$. [b] $w = 1/[\sigma^2(F_o^2) + (0.0200P)^2 + 35.9373P]$. [c] $P = (F_o^2 + 2F_c^2)/3$.

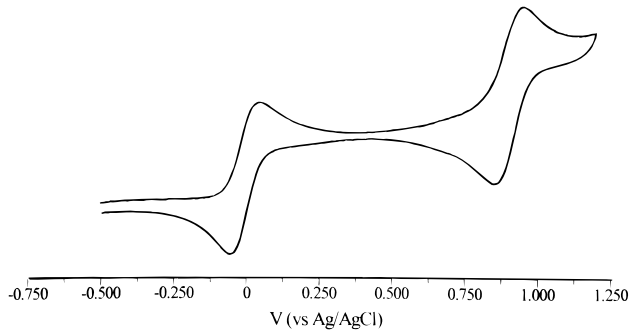

Figure 2. Cyclic voltammogram of **1** in CH_2Cl_2/0.5 M [n-Bu$_4$N]BF$_4$ at a Pt microelectrode (0.5 mm diameter) and a scan rate of 50 mV s^{-1}.

Results and Discussion

Following standard procedures for the synthesis of quadruply bonded molybdenum dimers,[1,9] treatment of $Mo(CO)_6$ under nitrogen with 1,2,3-triphenylguanidine in dry bis(2-methoxyethyl) ether (diglyme) under reflux for 6 h gave, on cooling, a yellow microcrystalline deposit of [Mo$_2${μ-η^2-(NPh)$_2$CNHPh}$_4$] (**1**) in 48% yield. The ^{1}H and ^{13}C NMR and +FAB mass spectra of **1** are consistent with this formulation. In air, crystalline **1** darkens from yellow to green and finally to black over a period of 1 h, while in solution it is considerably more air sensitive. This behavior contrasts with that of the similar complex with *p*-tolylformamidino ligands [RNCHNR]$^-$ (R = *p*-tolyl) which is stable in air and is only oxidized to the monocation at $E_{1/2} = +0.21$ V *vs* Ag/AgCl in CH_2Cl_2.[10] The guanidino ligand therefore appears to be superior at stabilizing the oxidized species compared to the amidino ligand, and this is confirmed by the cyclic voltammetric behavior of **1** in CH_2Cl_2, which shows two one-electron reversible oxidation waves at −0.05 and +0.85 V *vs* Ag/AgCl (Figure 2). Stirred voltammetry at 10 mV s^{-1} confirmed the oxidative nature of both these processes. The deep red monocation [Mo$_2${μ-η^2-(NPh)$_2$CNHPh}$_4$]$^+$ (**2**) and the dark blue dication [Mo$_2${μ-η^2-(NPh)$_2$CNHPh}$_4$]$^{2+}$ (**3**) may be obtained by chemical oxidation of **1** with silver tetrafluoroborate or ammonium cerium(IV) nitrate, respectively, or alternatively by bulk electrolysis of **1** at 0.2 and 1.1 V, respectively. Either method provides materials with cyclic voltammetric responses identical to that exhibited by **1**. Attempts to obtain crystalline samples of **3** have so far been hampered by reduction to **2** during crystallization.

Spectroelectrochemical studies of the oxidation processes reveal clean conversions of **1** to **2** and **2** to **3** with sharp isosbestic points apparent in the electronic absorption spectra in the UV/visible region (Figures 3 and 4). The UV/vis spectrum of **1** in CH_2Cl_2 is dominated by a broad absorption

(5) Cosier, J.; Glazer, A. M. *J. Appl. Crystallogr.* **1986**, *19*, 105.
(6) Altomare, A.; Cascarano, G.; Giacovazzo, C.; Guagliardi, A. *J. Appl. Crystallogr.* **1993**, *26*, 343.
(7) Sheldrick, G. M. *Shelxtl*; Siemens Analytical X-ray Instruments Inc.: Madison, WI, 1995.
(8) van der Sluis, P.; Spek, A. L. *Acta Crystallogr.* **1990**, *A46*, 194.
(9) Brignole, A. B.; Cotton, F. A. *Inorg. Synth.* **1972**, *13*, 81.
(10) Cotton, F. A.; Feng, X.; Matusz, M. *Inorg. Chem.* **1989**, *28*, 594.

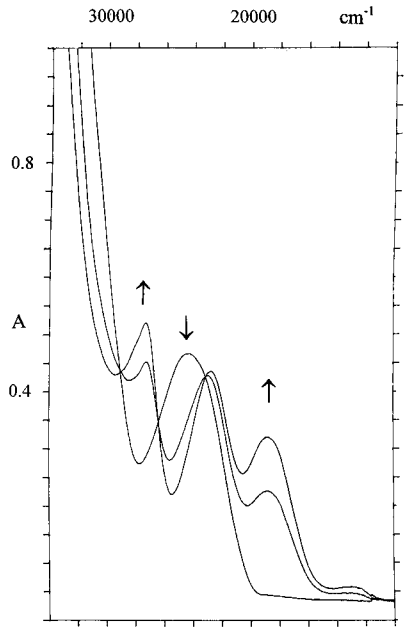

Figure 3. UV/vis spectroelectrochemical study of the conversion of **1** to **2**.

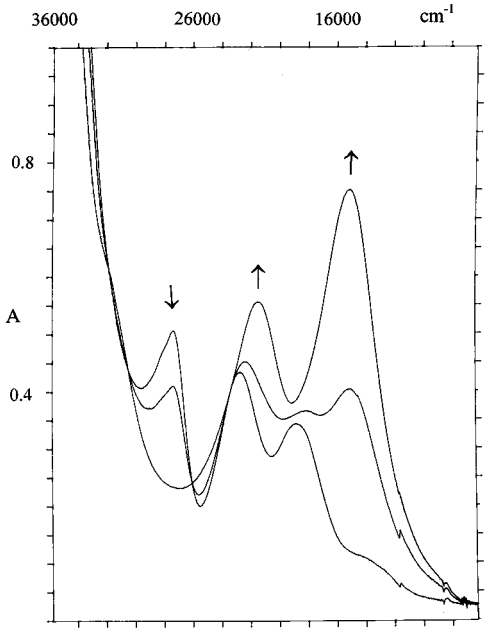

Figure 4. UV/vis spectroelectrochemical study of the conversion of **2** to **3**.

band at 24 370 cm^{-1}. According to the molecular orbital treatment of Cotton *et al*. performed on the related $[Mo_2(formamidinate)_4]$ and $[Mo_2(formamidinate)_4]^+$ species,[10] this visible band may be confidently assigned to the $\delta \rightarrow \delta^*$ transition within the Mo−Mo orbital manifold. Careful inspection of the spectrum of **1** also reveals two shoulders at 30 000 and 35 000 cm^{-1} which can be assigned to electronically allowed charge transfer transitions from predominantly ligand-based orbitals to the metal δ^* and π^* orbitals, respectively.

After removal of one electron from the δ orbital, the UV/vis spectrum increases considerably in complexity. The low-energy region of the spectrum has four transitions at 11 900, 18 900, 22 710, and 27 320 cm^{-1}. The weak lowest energy band at 11 900 cm^{-1} should be assigned to the $\delta \rightarrow \delta^*$ transition. The large shift in energy of this band when one electron is removed from the δ orbital is a consequence of the huge increase in Mo−Mo separation which accompanies the oxidation (*vide infra*).

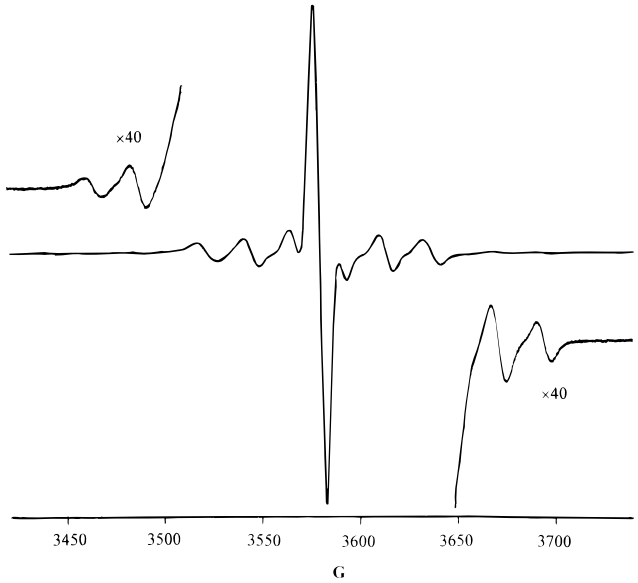

Figure 5. X-Band EPR spectrum of **2** in CH_2Cl_2. $\nu = 9.79$ GHz, $T = 293$ K, $g_{iso} = 1.943$, $A_{iso} = 20.5 \times 10^{-4}$ cm^{-1}.

Such an increase will result in less efficient overlap of the Mo-based *d* orbitals and therefore in decreased energy differences between the molecular orbitals. The three further bands at 18 900, 22 710, and 27 320 cm^{-1} are assigned to charge transfer transitions from ligand-based orbitals to the metal-based δ, δ^*, and π^* orbitals, respectively. These transitions are expected to have a higher intensity than the $\delta \rightarrow \delta^*$ transitions, which is as observed experimentally. Further metal-based transitions such as $\pi \rightarrow \delta$ are expected to occur in the visible region of the spectrum; however, their predicted intensity means that they will be obscured by the charge transfer bands.

Finally, the spectrum of **3** exhibits two intense bands at 15 010 and 21 400 cm^{-1}. The intensity of these bands is indicative of charge transfer transitions from the ligands to metal-based orbitals, in particular to the δ and δ^* orbitals. The δ orbital in **3** is unfilled, and hence there will be no low-energy $\delta \rightarrow \delta^*$ transition observable. The $\pi \rightarrow \delta$ transition is expected to occur at approximately the same energy as the ligand $\rightarrow \delta$ transition and cannot be individually distinguished because of its reduced intensity. The relatively small shift in the ligand to metal charge transfer transitions from **2** to **3** suggests that the Mo−Mo separation in **3** will be similar to that in **2**.

The CH_2Cl_2 solution EPR spectrum of **2** shows the expected signal pattern arising from the superposition of spectra due to the presence of isotopomers containing zero, one, or two of the $I = {}^5/_2$ molybdenum isotopes ^{95}Mo and ^{97}Mo (natural abundances 15.9% and 9.6%, respectively) as shown in Figure 5. To our knowledge, such fluid-solution EPR spectra were not obtainable from the other $[Mo_2]^{5+}$ systems so far characterized.[10−13] The frozen glass spectrum of **2** at 77 K (see Supporting Information) is different from those obtained from the analogous systems bridged by $[SO_4]^{2-}$ or $[C_3H_7CO_2]^-$ ligands.[11,12] It shows an axial type pattern with a larger component of the metal hyperfine matrix along the unique parallel direction, as is empirically expected for the unpaired electron primarily located in the δ orbital of the Mo−Mo bonding interaction. The metal hyperfine coupling values are smaller than those measured for these species, suggesting that

(11) Cotton, F. A.; Frenz, B. A.; Pedersen, E.; Webb, T. R. *Inorg. Chem.* **1975**, *14*, 391.
(12) Cotton, F. A.; Pedersen, E. *Inorg. Chem.* **1975**, *14*, 399. Cotton, F. A.; Pedersen, E. *J. Am. Chem. Soc.* **1975**, *97*, 303.
(13) Chang, I.-J.; Nocera, D. G. *J. Am. Chem. Soc.* **1987**, *109*, 4901.

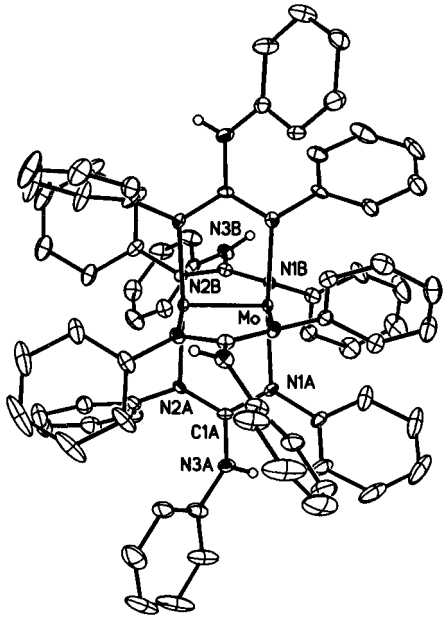

Figure 6. Molecular structure of $[Mo_2\{\mu\text{-}\eta^2\text{-}(NPh)_2CNHPh\}_4]$ (**1**). A crystallographic C_2 axis passing through the center of, and perpendicular to, the Mo−Mo vector relates the labeled to the unlabeled ligands.

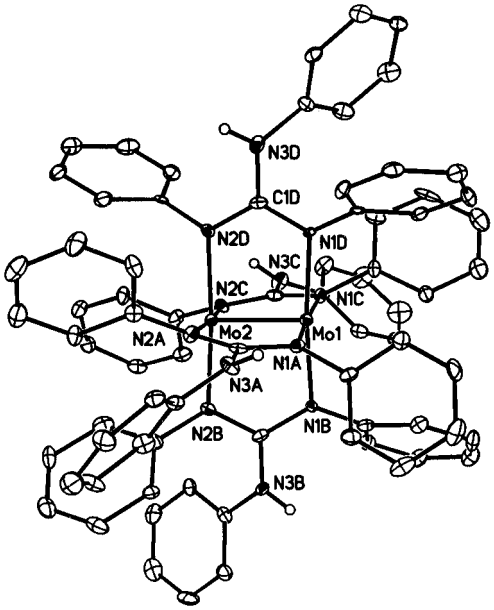

Figure 7. Molecular structure of the cation in $[Mo_2\{\mu\text{-}\eta^2(NPh)_2\text{-}CNHPh\}_4][BF_4]$ (**2**).

the molecular orbital containing the unpaired electron has less metal character and hence more ligand character than the SO_4^{2-} and $C_3H_7CO_2^-$-ligated complexes. It should also be noted that for **2** $g_{\|}$ is closer to g_e than $g_\perp$, which indicates that the electronic character of this species is different from that of $[Mo_2(SO_4)_4]^{3-}$ and $[Mo_2(C_3H_7CO_2)_4]^+$.

Single-crystal X-ray studies were carried out on **1** and **2**$[BF_4]$, and their structures are shown in Figures 6 and 7 respectively, and selected bond distances and angles for the two structures are provided in Tables 2 and 3. Both complexes adopt the paddlewheel structure typical for these tetrabridged molybdenum dimers and have Mo−Mo separations of 2.0839(9) and 2.2902(12) Å, respectively, an increase of 0.206(1) Å for the nominal reduction in bond order from 4 (σ^2, π^4, δ^2) to 3.5 (σ^2, π^4, δ). The N−Mo−Mo−N torsion angle also increases from 4.5 to 7.6° on oxidation. In the structures of both **1** and **2**, the phenyl groups attached to the coordinated nitrogens effectively block the Mo_2 dimer from axial ligation. Thus, although the unit cell of **1** contains diethyl ether, this is uncoordinated, and for **2** the shortest Mo−F (BF_4^-) distance is 6.035 Å.

Table 2. Selected Bond Distances (Å) for $[Mo_2\{\mu\text{-}\eta^2\text{-}(NPh)_2CNHPh\}_4]$ (**1**)

Mo−Mo	2.0839(9)	C(1A)−N(2A)	1.331(7)
Mo−N(1A)	2.171(5)	C(1A)−N(3A)	1.410(7)
Mo−N(1B)	2.160(4)	C(1B)−N(1B)	1.341(6)
Mo−N(2A)	2.179(4)	C(1B)−N(2B)	1.338(7)
Mo−N(2B)	2.156(5)	C(1B)−N(3B)	1.378(7)
C(1A)−N(1A)	1.336(7)		

Table 3. Selected Bond Distances (Å) for the Cation of $[Mo_2\{\mu\text{-}\eta^2\text{-}(NPh)_2CNHPh\}_4][BF_4]$ (**2**)

Mo(1)−Mo(2)	2.2902(12)	C(1A)−N(3A)	1.379(11)
Mo(1)−N(1A)	2.137(7)	C(1B)−N(1B)	1.447(11)
Mo(1)−N(1B)	2.157(7)	C(1B)−N(2B)	1.425(11)
Mo(1)−N(1C)	1.153(7)	C(1B)−N(3B)	1.357(10)
Mo(1)−N(1D)	2.138(7)	C(1C)−N(1C)	1.410(11)
Mo(2)−N(2A)	2.121(7)	C(1C)−N(2C)	1.338(11)
Mo(2)−N(2B)	2.159(7)	C(1C)−N(3C)	1.383(11)
Mo(2)−N(2C)	2.126(7)	C(1D)−N(1D)	1.399(11)
Mo(2)−N(2D)	2.140(7)	C(1D)−N(2D)	1.433(11)
C(1A)−N(1A)	1.434(11)	C(1D)−N(3D)	1.378(11)
C(1A)−N(2A)	1.385(11)		

In the crystal structure of **1** there is a crystallographic C_2 axis through the center of, and perpendicular to, the Mo−Mo vector, resulting in only two independent ligands. The resulting four Mo−N distances do not vary significantly and range from 2.156(5) to 2.179(4) Å. The CN_3 units of the ligands are essentially planar, with the C−N−C angles totaling 360°. In the structures of both **1** and **2**, the hydrogens on the nonligating nitrogens were located in Fourier difference maps, and although the uncertainties in their positions are large, it is apparent that these nitrogens are also essentially planar. For **1**, the angles around N(3A) and N(3B) total 355(7) and 359(7)°, respectively; however, it appears that this is due to delocalization of the nitrogen lone pair into the attached phenyl group rather than into the ligand, since the torsion angles between the respective ligand planes and N(3A)−C(31A) and N(3B)−C(31B) are large [55.3(8) and 42.7(8)°, respectively]. This conclusion is also supported by examination of the internal C−N distances of the ligands where the bonds to the uncoordinated nitrogens [1.410(7) and 1.378(7) Å] are found to be longer than those to the ligating ones [range 1.331(7)−1.338(7) Å], thus indicating a predominant contribution from resonance form **A** (Figure 1).

A comparison of the metrical parameters for the ligands in the two structures also reveals some evidence for an increased contribution from **B** (Figure 1) in the oxidized compound **2**. Although the differences between the central carbon to uncoordinated nitrogen bond distances for the two structures are not crystallographically significant, if these bond lengths are compared with those between the ligand central carbon atoms and the ligating nitrogens for each structure, the expected correlation appears: as pointed out above, for **1** these distances tend to be shorter than for the C−NHPh bonds, while for the structure of the oxidized complex **2** they range from 1.385(11)−1.447(11) Å as compared with a range of 1.357(10) to 1.383(11) for the C−NHPh bonds. Also significant is the observation that the torsion angles about the uncoordinated ligand nitrogens discussed above are smaller in the structure of **2** and range from 31(1) to 37(1)°.

While the Mo$\overset{4}{-}$Mo bond distance in **1** is typical for such systems, the value of 2.2902(12) Å for the Mo−Mo interaction with formal bond order of 3.5 in **2** is exceptionally large and should be compared with formal *triple*-bond (σ^2, π^4) lengths in the tetrabridged systems $[Mo_2(HEO_4)_4]^{2-}$ of 2.223(2) Å (E =

P)[14] and 2.265(1) Å (E = As).[15] There are only two other structurally characterized redox pairs of this type: the previously mentioned formamidinate complexes $[Mo_2\{(N\text{-}p\text{-tolyl})_2CH\}_4]^{0/+}$ and $[Mo_2(SO_4)_4]^{4-/3-}$, in which the increases in Mo−Mo distances observed on oxidation are 0.037(5) and 0.056(2) Å, respectively.[10,12] The contrast between the formamidinate complexes and the present examples is striking given that, apart from substitution of *p*-tolyl by phenyl, the ligand only differs in the replacement of the formamidinate −H with an −NHPh group.

Further work is underway to establish the origin of this Mo−Mo bond lengthening effect; however, at this stage we are of the opinion that it must be associated with the increased donor ability (basicity) of the guanidino ligand as compared with the formamidino ligand, by virtue of a contribution from resonance form **B** (Figure 1). This does however, conflict with the rationalization put forward by Cotton in accounting for the smaller difference in Mo−Mo separation in the $[Mo_2\{(N\text{-}p\text{-tolyl})_2CH\}_4]^{0/+}$ redox pair as compared with that found for the $[Mo_2(SO_4)_4]^{4-/3-}$ species. This effect was seen as an attenuation of the natural contraction of metal d orbitals, and consequent weakening of the metal−metal bond, concomitant with oxidation by the greater basicity of the formamidinate ligand.[10] The consistent application of this explanation to account for various other observed bond length trends in metal−metal multiply bonded species lends further validity to this argument.[16] In the present case, the electrochemical studies clearly suggest a greater basicity for the guanidino ligand as compared with the formamidinate, and thus, on the basis of the above argument, an increase in Mo−Mo separation somewhat less than 0.037 Å would be predicted on oxidation from **1** to **2**. This is clearly inconsistent with the increase of 0.206(1) Å observed for this process, and a full explanation must await a detailed analysis of the bonding in these systems. However, we suggest that one possible explanation which does not impugn the effect put forward by Cotton, but rather swamps it, is the involvement of a ligand π-donor contribution to N−Mo bonding. Such an interaction between an occupied π-symmetry orbital on the nitrogen donors of resonance form **B** of the ligand and the antibonding combination of Mo $d_{x^2-y^2}$ orbitals would populate the π^* orbital of the Mo−Mo interaction and thus further weaken the bond. A significant π-donation of this type is only possible for the **B** resonance contribution, since in **A** the occupied π-symmetry orbitals are involved in C−N π-bonding in the N−C−N diazaallyl fragment of the ligand, while in **B** the donor nitrogens are effectively of the amide type NR_2^-. The observation that the total loss of δ-bonding from the quadruply bonded dimers $[Mo_2Cl_4(diphosphine)_2]$, estimated by characterization of both eclipsed and staggered examples, leads to an increase in Mo−Mo separation of *ca*. 0.10 Å[17] is a further indication that a bond lengthening mechanism additional to the depopulation of the Mo−Mo δ-bonding orbital is operating in the conversion of **1** to **2**. This becomes particularly evident when it is realized that an increase of twice this magnitude is found for removal of just one δ-electron.

Conclusions

The 1,2,3-triphenylguanidino ligand $[(PhN)_2CNHPh]^-$ has been shown by this study to be exceptionally flexible with regard to its ability to stabilize a range of oxidation levels in the dimolybdenum system. This has enabled the characterization of such complexes in three oxidation levels, $[Mo_2]^{4+/5+/6+}$. Further work is underway to investigate the properties of systems in which the proton on the uncoordinated nitrogen has been removed and thus involve guanidine dianion ligands.

Acknowledgment. We thank the Engineering and Physical Science Research Council (EPSRC) for a studentship (L.A.M.) and provision of a four-circle diffractometer and The Royal Society, The Leverhulme Trust, and The Nuffield Foundation for financial support.

Supporting Information Available: The frozen solution (CH_2Cl_2/toluene, 77 K) EPR spectrum of **2**$[BF_4]$ (1 page). X-ray crystallographic files, in CIF format, for compounds **1** and **2**$[BF_4]$ are available on the Internet only. Access and ordering information is given on any current masthead page.

IC960712J

(14) Bino, A.; Cotton, F. A. *Angew. Chem., Int. Ed. Engl.* **1979**, *18*, 462.
(15) Ribas, J.; Poilblanc, R.; Sourisseau, C.; Solans, X.; Brianso, J. L.; Miravitlles, C. *Transition Met. Chem.* **1983**, *8*, 244.
(16) Cotton, F. A. *Chem. Soc. Rev.* **1983**, *12*, 35.
(17) Campbell, F. L.; Cotton, F. A.; Powell, G. L. *Inorg. Chem.* **1985**, *24*, 4384.